A Volume-of-Fluid Dual-Scale Approach for Simulating Turbulent Liquid/Gas Interactions

Dominic Kedelty[(✉)] , James Uglietta, and Marcus Herrmann

Arizona State University, Tempe, AZ 85284, USA
dkedelty@asu.edu
http://www.multiphase.asu.edu

Abstract. Advances to a dual-scale modeling approach (Gorokhovski and Herrmann, 2008) are presented to describe turbulent phase interface dynamics in a Large Eddy Simulation spatial filtering context. Spatial filtering of the governing equations to decrease the burden of Direct Numerical Simulation introduces several sub-filter terms that require modeling. Instead of developing individual closure models for the interface associated terms, the dual-scale approach uses an exact closure by explicitly filtering a fully resolved realization of the phase interface. This resolved realization is maintained on a high-resolution over-set mesh using a Refined Local Surface Grid approach (Herrmann, 2008) employing an un-split, geometric, bounded, and conservative Volume-of-Fluid method (Owkes and Desjardins, 2014). Advection of the phase interface on this DNS scale requires a reconstruction of the fully resolved interface velocity. This velocity is the sum of the filter scale velocities, readily available from an LES solver, and sub-filter velocity fluctuations. These fluctuations can be due to sub-filter turbulent eddies, which can be reconstructed on-the-fly using a local fractal interpolation technique (Scotti and Meneveau, 1999) to generate time evolving sub-filter velocity fluctuations. In this work, results from the dual-scale LES model are compared to DNS results for four different realizations of a unit density and viscosity contrast interface in a homogeneous isotropic turbulent flow at infinite Weber number. Introduction of a sub-filter turbulent velocity reconstruction in a passive scalar context is the first step towards use of a dual-scale model for multiphase applications.

Keywords: Volume-of-fluid · Dual-scale · Fractal interpolation · RLSG

1 Introduction

Atomization in turbulent environments involves a vast range of length and time scales. Predictive simulations aiming to resolve all relevant scales thus require

enormous computational resources, taxing even the most powerful computers available today [5]. Since primary atomization is governed by the dynamics of the interface, a need therefore exists for appropriate interface models that make the computational cost of predicting the atomization outcome more tractable.

A wide range of phenomenological models aiming to represent statistically the essential features of atomization have been proposed in the past. Although these aim to introduce the dominant mechanisms for breakup, they often use round blobs injected from the nozzle exit and hence neglect all details of the interface dynamics.

Other modeling approaches to atomization include stochastic models [6,7] representing the interface by constituent stochastic particles and the mean interface density transport equation model for Reynolds-Averaged Navier-Stokes (RANS) approaches [21,22]. The former treats the interface dynamics in a stochastic sense but requires the *a priori* knowledge of the breakup mechanism, whereas the latter is affected by the drawbacks of the RANS approach: the transport of the mean interface density is modeled by a diffusion-like hypothesis, thereby neglecting the spatial grouping effects of liquid elements [5].

In the context of Large Eddy Simulations (LES), [12,18–20] have proposed models to close the unclosed terms arising from the introduction of spatial filtering into the governing equations. However, these models typically neglect the contribution of the sub-filter surface tension term and are based on a cascade process hypothesis that may be questionable in the context of surface tension-driven atomization. An exception is the model for the sub-filter surface tension term proposed in [1]. In [9,11], a dual-scale approach for LES of interface dynamics was proposed and a model for the sub-filter surface tension induced motion of phase interfaces was developed.

The purpose of this contribution is to develop a model for the sub-filter phase interface motion induced by sub-filter turbulent velocity fluctuations. Combining such a model with the surface tension model proposed in [9,11] will result in a LES model applicable to atomizing flows.

2 Governing Equations

The equations governing the fully resolved motion of an unsteady, incompressible, immiscible, two-fluid system in the absence of surface tension are the Navier-Stokes equations,

$$\frac{\partial \rho \boldsymbol{u}}{\partial t} + \nabla \cdot (\rho \boldsymbol{u} \otimes \boldsymbol{u}) = -\nabla p + \nabla \cdot \left(\mu \left(\nabla \boldsymbol{u} + \nabla^T \boldsymbol{u} \right) \right) , \tag{1}$$

where $\boldsymbol{u}$ is the velocity, ρ the density, p the pressure, and μ the dynamic viscosity. Here, we neglect surface tension to solely focus on the turbulence induced dynamics of phase interfaces. Furthermore, the continuity equation results in a divergence-free constraint on the velocity field

$$\nabla \cdot \boldsymbol{u} = 0 . \tag{2}$$

Assuming ρ and μ are constant within each fluid, density and viscosity can be calculated from

$$\rho = \psi\rho_l + (1-\psi)\rho_g \tag{3}$$

$$\mu = \psi\mu_l + (1-\psi)\mu_g\,, \tag{4}$$

where indices l and g denote values in liquid and gas, respectively, and ψ is a volume-of-fluid scalar that is $\psi = 0$ in the gas and $\psi = 1$ in the liquid with

$$\frac{\partial\psi}{\partial t} = -\boldsymbol{u}\cdot\nabla\psi = -\nabla\cdot(\boldsymbol{u}\psi) + \psi\nabla\cdot\boldsymbol{u}\,. \tag{5}$$

Here, the last term on the right-hand side is zero for incompressible flows, see Eq. (2). In this work, unit density and viscosity ratios are considered making this a single-phase flow, therefore Eqs. (3) and (4) are unnecessary but are included for completeness sake.

2.1   Filtered Governing Equations

Introducing spatial filtering into Eqs. (1) and (2) and assuming that the filter commutes with both the time and spatial derivatives, the filtered governing equations can be derived [20],

$$\frac{\partial\overline{\rho}\,\overline{\boldsymbol{u}}}{\partial t} + \nabla\cdot(\overline{\rho}\overline{\boldsymbol{u}}\otimes\overline{\boldsymbol{u}}) = -\nabla\overline{p} + \nabla\cdot(\overline{\mu}(\nabla\overline{\boldsymbol{u}}+\nabla^T\overline{\boldsymbol{u}})) + \boldsymbol{\tau}_1 + \nabla\cdot(\boldsymbol{\tau}_2+\boldsymbol{\tau}_3)\,, \tag{6}$$

$$\nabla\cdot\overline{\boldsymbol{u}} = 0\,, \tag{7}$$

where $^-$ indicates spatial filtering, and

$$\boldsymbol{\tau}_1 = \frac{\partial\overline{\rho}\,\overline{\boldsymbol{u}}}{\partial t} - \frac{\partial\overline{\rho\boldsymbol{u}}}{\partial t} \tag{8}$$

$$\boldsymbol{\tau}_2 = \overline{\rho}\,\overline{\boldsymbol{u}}\otimes\overline{\boldsymbol{u}} - \overline{\rho\boldsymbol{u}\otimes\boldsymbol{u}} \tag{9}$$

$$\boldsymbol{\tau}_3 = \overline{\mu(\nabla\boldsymbol{u}+\nabla^T\boldsymbol{u})} - \overline{\mu}(\nabla\overline{\boldsymbol{u}}+\nabla^T\overline{\boldsymbol{u}})\,, \tag{10}$$

where $\boldsymbol{\tau}_1$, $\boldsymbol{\tau}_2$, and $\boldsymbol{\tau}_3$ are associated, respectively, with acceleration, advection, and viscous effects [20]. Using Eqs. (3) and (4), the filtered density and viscosity in Eq. (6) are

$$\overline{\rho} = \rho_l\overline{\psi} + \rho_g(1-\overline{\psi}) \tag{11}$$

$$\overline{\mu} = \mu_l\overline{\psi} + \mu_g(1-\overline{\psi})\,, \tag{12}$$

where

$$\overline{\psi} = \int\mathcal{G}(\boldsymbol{x})\psi d\boldsymbol{x}\,, \tag{13}$$

and $\mathcal{G}$ is a normalized spatial filter function.

3   The Dual-Scale Approach to Modeling Sub-filter Interface Dynamics

Instead of relying on a cascade process by which dynamics on a sub-filter scale can be inferred from the dynamics on the resolved scale, the dual-scale approach proposed in [11] aims to maintain a fully resolved realization of the immiscible interface geometry at all times, expressed, for example, in terms of a volume-of-fluid scalar ψ. Then $\overline{\psi}$ can be calculated exactly by explicit filtering using Eq. (13).

Although this is an exact closure, the problem of modeling is of course simply shifted to the problem of maintaining a fully resolved realization of the interface geometry, i.e., describing the fully resolved motion of the interface, Eq. (5). Since the fully resolved velocity is the sum of the filtered velocity and the sub-grid velocity, $\boldsymbol{u} = \overline{\boldsymbol{u}} + \boldsymbol{u}_{sg}$, this results in

$$\frac{\partial \psi}{\partial t} = -\nabla \cdot \left(\left(\overline{\boldsymbol{u}} + \boldsymbol{u}_{sg} \right) \psi \right) + \psi \nabla \cdot \left(\overline{\boldsymbol{u}} + \boldsymbol{u}_{sg} \right), \tag{14}$$

where the only term requiring modeling is $\boldsymbol{u}_{sg}$. In [11], a model for $\boldsymbol{u}_{sg}$ is proposed consisting of three contributions,

$$\boldsymbol{u}_{sg} = \boldsymbol{u}' + \delta \boldsymbol{u} + \boldsymbol{u}_{\sigma}, \tag{15}$$

where $\boldsymbol{u}'$ is due to sub-filter turbulent eddies, $\delta \boldsymbol{u}$ is attributed to the interface velocity increment due to relative sub-filter motion between the two immiscible fluids, and $\boldsymbol{u}_{\sigma}$ is due to sub-filter velocities induced by sub-filter surface tension forces. The focus of the current contribution is on the first term; for a modeling outline of the second term, the reader is referred to [10,11], and for modeling of the last term, the reader is referred to [9].

3.1   Sub-filter Turbulent Fluctuation Velocity Models

We propose to reconstruct the sub-filter turbulent fluctuation velocity $\boldsymbol{u}'$ using fractal interpolation [17]. To demonstrate fractal interpolation in one dimension, consider 3 adjacent LES scale nodes x_0, x_1, and x_2 with velocities $\overline{u}_0$, $\overline{u}_1$, and $\overline{u}_2$. Following [4,17] the fractal interpolation operator $\mathcal{W}_{FI}$ can be written as

$$\mathcal{W}_{FI}(x) = \overline{u}_0 + \frac{\overline{u}_1 - \overline{u}_0}{x_1 - x_0}(x - x_0)$$
$$+ d_1 \left(u(2x - x_0) - \overline{u}_0 - \frac{\overline{u}_2 - \overline{u}_0}{x_2 - x_0}(2x - x_0) \right) \text{ if } x \in [x_0, x_1] \tag{16}$$

$$\mathcal{W}_{FI}(x) = \overline{u}_1 + \frac{\overline{u}_2 - \overline{u}_1}{x_2 - x_1}(x - x_1)$$
$$+ d_2 \left(u(2x - x_0) - \overline{u}_0 - \frac{\overline{u}_2 - \overline{u}_0}{x_2 - x_0}(2x - x_0) \right) \text{ if } x \in [x_1, x_2] \tag{17}$$

Here $|d_1| < 1$ and $|d_2| < 1$ are stretching factors making $\mathcal{W}_{FI}$ a contractive mapping [17]. Successively applying the fractal interpolation operator $\mathcal{W}_{FI}$ starting with the LES filter velocities, generates the fully resolved turbulent fluctuation velocity. In order to extend the method into three dimensions, the fractal interpolation operator is first performed in one spatial direction only, followed by separate 1D fractal interpolations in the other two directions [17].

The determination of the values of the stretching factors d_1 and d_2 follows the so-called ZE1 model of [17] by using $d_1 = -d_2 = \pm 2^{-1/3}$ with the sign chosen randomly with equal probability. This choice of d_i generates a velocity signal that satisfies the $-5/3$ kinetic energy spectrum of turbulence at all sub-filter scales.

4   Numerical Methods

Equation (14) is solved using an unsplit geometric transport scheme for volume-of-fluid scalars that ensures both discrete volume conservation of each fluid and boundedness of the volume-of-fluid scalar, ψ [13]. Geometric reconstruction of the interface within each computational cell is done using PLIC reconstruction, employing analytical formulas [16] using ELVIRA estimated normals [14, 15].

To efficiently solve Eq. (14) for the fully resolved immiscible interface, the RLSG method [8] is employed. By design, it solves the interface capturing advection equation on a separate, highly resolved Cartesian overset grid of mesh spacing h_G, independent of the underlying LES flow solver grid of mesh spacing h. In the dual-scale LES approach, h_G needs to be chosen sufficiently small to maintain a fully resolved realization of the phase interface.

The velocity $\boldsymbol{u}$ at RLSG scale h_G is calculated from

$$\boldsymbol{u} = \mathcal{W}_{FI}^k \overline{\boldsymbol{u}}, \tag{18}$$

where the superscript k indicates k-times application of the fractal interpolation operator $\mathcal{W}_{FI}$, with

$$k = \frac{\log\left(\frac{h}{h_G}\right)}{\log(2)}. \tag{19}$$

Since the LES flow solver used in this work utilizes a staggered mesh layout, the face normal velocities in each spatial direction are not co-located and hence the fractal interpolation has to be performed for different locations depending on the spatial component of the velocity vector.

The unsplit, geometric advection scheme of [13] requires face-centered velocities that are discretely divergence-free to ensure both conservation and boundedness. While discretely divergence free filtered velocities $\overline{\boldsymbol{u}}$ are available on the flow solver mesh in a standard fractional step method, i.e., $\nabla_h \cdot \overline{\boldsymbol{u}} = 0$, the fractal interpolated velocities $\boldsymbol{u}$ are not necessarily divergence free on the fine overset mesh. To ensure $\nabla_{h_G} \cdot \boldsymbol{u} = 0$, $\boldsymbol{u}$ is projected into the subspace of solenoidal velocity fields using the projection/correction step of a standard fractional step method applied to the overset mesh contained within each LES cell separately.

Note that the resulting Poisson systems that need to be solved to determine the Lagrange multiplier for projection of $\boldsymbol{u}$ are defined on a per LES cell basis, necessitating an additional step to make the LES cell face average of $\boldsymbol{u}$ equal to the LES scale filtered velocity $\overline{\boldsymbol{u}}$. This is achieved by computing and applying a per cell face constant correction velocity to $\boldsymbol{u}$, similar to the approach used to determine an outlet correction velocity in the fractional step method to make the approach satisfy the continuity equation on the entire domain. Here the correction velocity applied to each cell face ensures satisfying the continuity equation for u on the LES filter scale h.

The fractal interpolation reconstruction is performed at every LES time step such that the resolved scale velocity $\boldsymbol{u}$ is actively evolving with the LES velocity $\overline{\boldsymbol{u}}$ on the LES time scale.

Finally, to calculate $\overline{\psi}$, Eq. (13) is evaluated by setting the filter size to the local flow solver mesh spacing h and evaluating the integral by explicitly summing the volume-of-fluid scalar ψ of those overset-mesh cells that are contained within a given LES flow solver cell.

4.1 Comparison Metrics

Assuming that the phase interface is initially planar with normal orientation in the y-direction, we define $\alpha(x, z, t)$ as the liquid volume fraction that is contained within a square column in the y-direction with cross sectional area equal to h_G^2. Using the definition of $\alpha(x, z, t)$, the RMS sum of the time evolution of α can be defined as

$$\alpha_0'(t) = \sqrt{\frac{1}{L^2} \int_L \int_L \left((\alpha(x, z, t) - \alpha(x, z, 0))^2 \, dx dz \right.}. \tag{20}$$

This quantity depends predominantly on the large scale movement of the interface. Defining $\overline{\alpha}(x, z, t)$ as the liquid volume fraction contained within a square column in the y-direction with cross sectional area equal to the LES filter scale h^2, we define the sub-filter liquid column height RMS as

$$\alpha'(t) = \sqrt{\frac{1}{L^2} \int_L \int_L \left((\alpha(x, z, t) - \overline{\alpha}(x, z, t))^2 \, dx dz \right.}, \tag{21}$$

This quantity depends predominantly on the sub-filter transport of the volume fraction.

To take into account that even on an LES mesh scale, the PLIC reconstruction of the filtered phase interface geometry provides a level of sub-filter geometry resolution beyond the mere liquid column height $\overline{\alpha}$, we define a local quantity C_{mix} that measures the sub-filter variation of the phase interface on the overset mesh compared to the LES mesh. C_{mix} is calculated by first performing a PLIC reconstruction on the LES mesh using the filtered volume fraction $\overline{\psi}$, see Fig. 1. The reconstructed planar representation of the phase interface is then used to calculate liquid volume fractions on the overset mesh $\overline{\psi}_{h_G}$. The root mean square
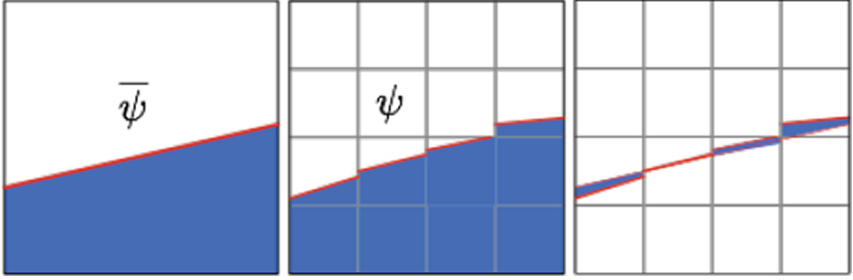
Fig. 1. PLIC geometry on LES mesh cell (left), fully resolved PLIC geometry (center), difference used to calculate C_{mix} (right).
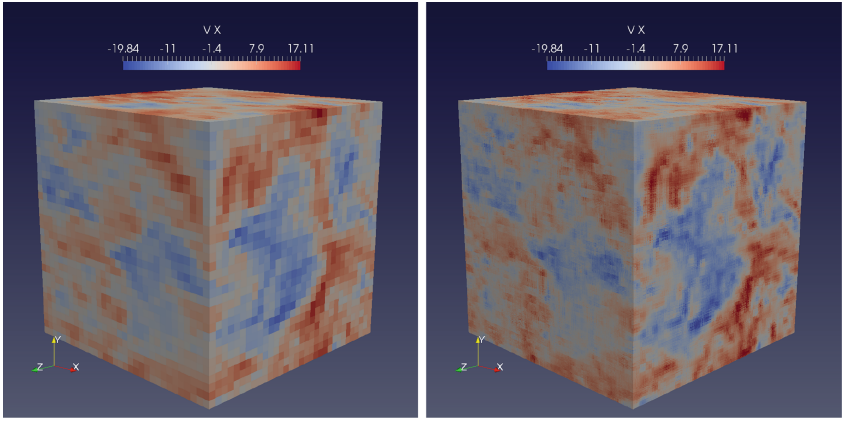
Fig. 2. Comparison of LES filtered velocity (left) and fractal interpolated velocity (right).

of the difference of these volume fractions and the fully resolved volume fractions ψ, see Fig. 1, is C_{mix},

$$C_{mix}(t) = \sqrt{\frac{1}{L^3} \int_L \int_L \int_L \left(\psi - \overline{\psi}_{h_G}\right)^2 dxdydz}. \tag{22}$$

It should be pointed out that both α' and C_{mix} will remain zero for all time without a dual-scale model.

The probability density function (PDF) of interface curvature is used as a final comparison metric. The curvature that is sampled is the mean curvature calculated by height function [3]. Samples are taken from every RLSG cell that contains an interface and $|\kappa|$ is used to create the PDF.
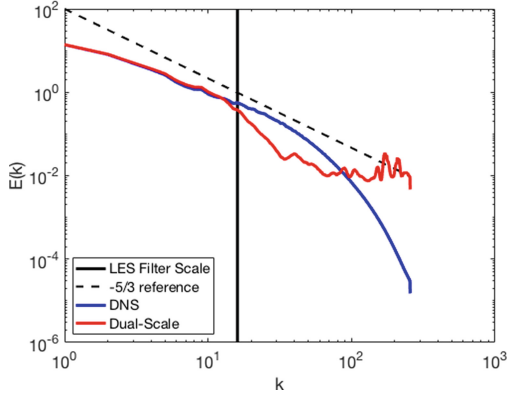
Fig. 3. Resulting 3D spatial kinetic energy spectra for 512^3 overset mesh using fractal interpolation (red). DNS (blue) and $-5/3$ reference line (dashed) are also provided. Vertical solid black line denotes the LES filter scale.

5   Results and Discussion

An initially flat interface is placed inside a box of fully developed isotropic turbulence. The fully developed isotropic turbulence field was graciously provided by R. Chiodi and O. Desjardins [2]. Both density and viscosity ratio are unity, and no surface tension forces are present with a Reynolds number of $Re_\lambda = 156$ and $We_\lambda = \infty$. Here, we present DNS and LES results using the dual-scale approach employing a LES mesh resolution of 32^3 and an overset mesh resolution of 512^3 for four different realizations generated by placing the phase interface at different initial heights in the turbulent velocity field. The four different initial heights listed from realization 1–4 are $y = \pi, y = \pi/2, y = 0, y = 3\pi/2$. DNS results were obtained using a 512^3 mesh for both the flow solver and interface advection scheme.

Figure 2 shows, as an example, a comparison of the LES filtered velocity field and the fractal interpolated velocity. Noticeably more small scale structure is visible in the fractal interpolated velocity compared to the filter scale LES velocity. This is corroborated by the kinetic energy spectrum shown in Fig. 3 that compares the kinetic energy spectrum of the fractal interpolated velocities to the DNS velocities. The fractal interpolation kinetic energy spectrum does show a noticeable dip before beginning to follow the $-5/3$ energy cascade. Note the absence of any viscous dissipation range in the fractal interpolated velocities.

Figure 4 compares one realization of the phase interface geometry using fractal interpolation and the interface geometry that would be obtained without any dual-scale model. Including the fractal interpolated sub-filter velocity in the advection velocity of the resolved realization of the interface clearly leads to significantly more surface corrugations, as expected.

Figure 5a–b shows the liquid column height RMS α_0' with respect the initially flat interface. In Fig. 5a, comparison of the four different realizations show a large
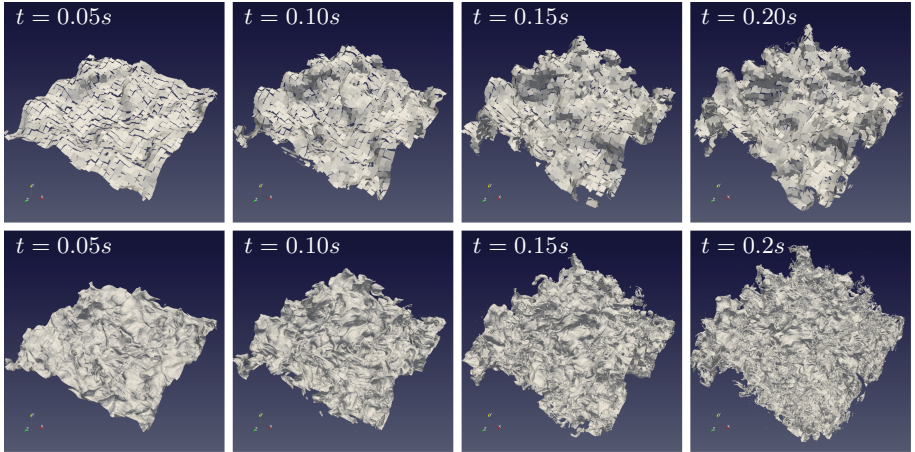
Fig. 4. Comparison of time evolving phase interface geometry for Realization #1 of homogeneous isotropic turbulence at several time steps: no dual-scale model (top) and fractal interpolation velocity (bottom).

effect on α'_0, because α'_0 depends strongly on the large scale motion of the interface that are noticeably different from realization to realization. However, each of the individual LES results shows very good agreement with its corresponding DNS result. Figure 5b compares the LES results with and without dual-scale model to the DNS results for one realization. It can be seen that the dual-scale LES result agrees more closely with the DNS, although the results without dual-scale model are not too different from the DNS results since α'_0 depends mostly on the large scale motion on the LES filter scale.

Figure 5c shows the sub-filter liquid column height RMS α' for the different realizations. The results presented are only shown until the periodic boundary condition in the interface normal direction impacts the measurement. The difference between the realizations is very small, consistent with the observation that α' is a sub-filter quantity exhibiting a degree of universality of the small scales. The dual-scale LES simulations consistently over-predict α' at later times compared to the DNS results. However, it should be noted that α' is always zero if no dual-scale LES model is applied and the dual-scale model is therefore a significant improvement.

Figure 5d compares the sub-filter variation C_{mix} for the different realizations. Again, the difference between the realizations is small, indicating that C_{mix} is a sub-filter quantity that exhibits a degree of universality on the small scales. The dual-scale LES simulations consistently under-predict C_{mix} compared to the DNS results. However, again it should be noted that C_{mix} is always zero if no dual-scale LES model is applied and the dual-scale model is therefore a significant improvement.

Finally, Fig. 6 compares the PDF of interfacial curvature. Interestingly, no difference in the PDFs can be observed between the four different realizations
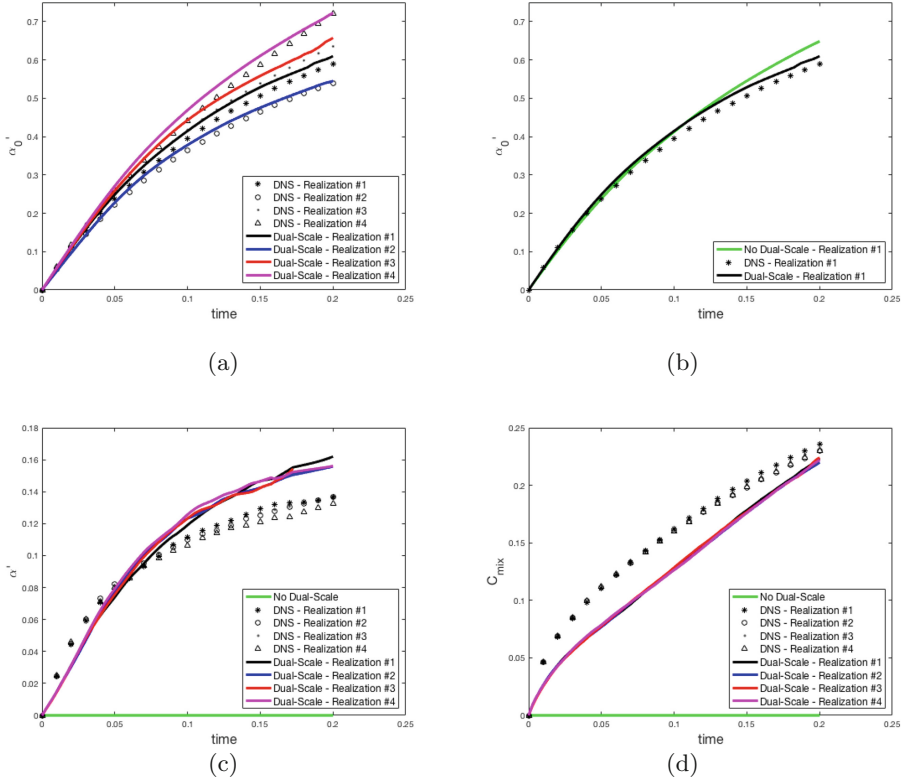
Fig. 5. Comparison of column height RMS α_0' for: (a) Different realizations of Re_λ. (b) No sub-filter velocity, DNS, and fractal interpolation. (c) Comparison of sub-filter liquid column height RMS α'. (d) Comparison Metric C_{mix}.

of Re_λ. While this is not surprising on the small scales, this also holds true for the larger scales as well. The dual-scale LES results show good agreement with the DNS results while the LES results without the dual-scale model are significantly different. Between $\kappa = 1/h$ and $\kappa = 1/h_G$ the dual-scale model overpredicts the population of curvature by approximately 1% as compared to the DNS results. Comparison of dual-scale LES and DNS results at $\kappa < 10^{-1}$, i.e., at radii of curvature that are larger than the computational box size of 2π, shows a difference of less than 0.01%. Note that both dual-scale LES and DNS results show a peak curvature probability at $\kappa = 1/h_G$, whereas the LES results without dual-scale model are limited to $\kappa = 1/h$. Since the present simulations are for infinite Weber number, the Hinze scale, aka Komogorov's critical radius, is zero and hence the appearance of larger and larger curvatures with time is only limited by the available mesh resolution.

It should be stressed that the dual-scale LES result using the time evolving fractal interpolation generates the same population of curvatures as the DNS and

hence it can be conjectured that the dual-scale LES model might generate similar droplet sizes in atomization cases, if drop generation is initiated by turbulent velocity fluctuations.
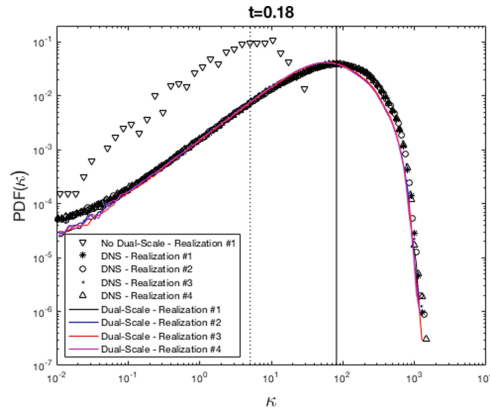
Fig. 6. Comparison of probability density function of curvature after the interface has had time to deform. Vertical reference lines denote the curvature of: $1/h_G$ (solid) $1/h$ (dotted).

6   Summary and Conclusions

A dual-scale modeling approach for phase interface dynamics in turbulent flows is presented that is based on a fractal interpolation technique to generate fully resolved turbulent velocity fields. The method uses overset high-resolution meshes to capture a resolved realization of the phase interface geometry that can be explicitly filtered to close the terms that require modeling in the filtered Navier-Stokes equations. Comparison of DNS and dual-scale LES results show good agreement for the case of an initially planar phase interface of unit density and viscosity contrast at infinite Weber number placed into a homogenous isotropic decaying turbulence field. This favorable comparison includes the probability density function of interfacial curvature, an earlier indicator that the proposed dual-scale LES model may be applicable to atomization cases where droplet generation is initiated by turbulent eddies.

The dual-scale method has also shown significant improvements in computational cost. Proper implementation of the dual-scale method can be orders of magnitude faster than a pure DNS simulation when only a small portion of the domain contains an interface, as is the case for primary atomization. In the case where the entire domain is filled with interface, the dual-scale method has shown to be as fast as pure DNS.

Future work will focus on incorporating the dual-scale model for surface tension and an analysis on the impact of sub-filter surface tension on the interface dynamics.

References

1. Aniszewski, W., Bogusławski, A., Marek, M., Tyliszczak, A.: A new approach to sub-grid surface tension for LES of two-phase flows. J. Comput. Phys. **231**(21), 7368–7397 (2012). http://www.sciencedirect.com/science/article/pii/S002199911 2003890
2. Chiodi, R., Desjardins, O.: DNS of turbulent phase interfaces (2017)
3. Cummins, S.J., François, M.M., Kothe, D.B.: Estimating curvature from volume fractions. Comput. Struct. **83**, 425–434 (2005)
4. Ding, K.Q., Zhang, Z.X., Shi, Y.P., She, Z.S.: Synthetic turbulence constructed by spatially randomized fractal interpolation. Phys. Rev. E **82**(3), 036311 (2010). https://doi.org/10.1103/PhysRevE.82.036311
5. Gorokhovski, M., Herrmann, M.: Modeling primary atomization. Annu. Rev. Fluid Mech. **40**(1), 343–366 (2008). http://arjournals.annualreviews.org/doi/abs/10.1146/annurev.fluid.40.111406.102200
6. Gorokhovski, M., Jouanguy, J., Chtab, A.: Simulation of air-blast atomization: "floating guard" statistic particle method for conditioning of LES computation; stochastic models of break-up and coalescence. In: Proceedings of International Conference on Liquid Atomization and Spray Systems (2006)
7. Gorokhovski, M., Jouanguy, J., Chtab, A.: Stochastic simulation of the liquid jet break-up in a high-speed air coflow. In: International Conference on Multiphase Flow, Leipzig, Germany (2007)
8. Herrmann, M.: A balanced force refined level set grid method for two-phase flows on unstructured flow solver grids. J. Comput. Phys. **227**(4), 2674–2706 (2008). http://www.sciencedirect.com/science/article/B6WHY-4R53WMC-7/2/bd0eb9d 6157d8845efeb734b0aa6a6cf
9. Herrmann, M.: A sub-grid surface dynamics model for sub-filter surface tension induced interface dynamics. Comput. Fluids **87**(0), 92–101 (2013). https://doi.org/10.1016/j.compfluid.2013.02.008. http://www.sciencedirect.com/science/article/pii/S0045793013000637
10. Herrmann, M., Gorokhovski, M.: An outline of a LES subgrid model for liquid/gas phase interface dynamics. In: Proceedings of the 2008 CTR Summer Program, pp. 171–181. Center for Turbulence Research, Stanford University, Stanford (2008)
11. Herrmann, M., Gorokhovski, M.: A large eddy simulation subgrid model for turbulent phase interface dynamics. In: ICLASS 2009, 11th Triennial International Annual Conference on Liquid Atomization and Spray Systems, Vail, CO (2009)
12. Labourasse, E., Lacanette, D., Toutant, A., Lubin, P., Vincent, S., Lebaigue, O., Caltagirone, J.P., Sagaut, P.: Towards large eddy simulation of isothermal two-phase flows: governing equations and a priori tests. Int. J. Multiphase Flow **33**(1), 1–39 (2007). http://www.sciencedirect.com/science/article/pii/S03019322 06000905
13. Owkes, M., Desjardins, O.: A computational framework for conservative, three-dimensional, unsplit, geometric transport with application to the volume-of-fluid (VOF) method. J. Comput. Phys. **270**, 587–612 (Aug 2014). https://doi.org/10.1016/j.jcp.2014.04.022, http://linkinghub.elsevier.com/retrieve/pii/S00219991140 0285X
14. Pilliod, J.E.: An analysis of piecewise linear interface reconstruction algorithms for volume-of-fluid methods. Master's thesis, University of California Davis (1992)

15. Pilliod Jr., J.E., Puckett, E.G.: Second-order accurate volume-of-fluid algorithms for tracking material interfaces. J. Comput. Phys. **199**(2), 465–502 (2004). https://doi.org/10.1016/j.jcp.2003.12.023. http://www.sciencedirect.com/science/article/pii/S0021999104000920

16. Scardovelli, R., Zaleski, S.: Analytical relations connecting linear interfaces and volume fractions in rectangular grids. J. Comput. Phys. **164**(1), 228–237 (2000). https://doi.org/10.1006/jcph.2000.6567. http://www.sciencedirect.com/science/article/pii/S0021999100965677

17. Scotti, A., Meneveau, C.: A fractal model for large eddy simulation of turbulent flow. Phys. D: Nonlinear Phenomena **127**(3–4), 198–232 (1999). https://doi.org/10.1016/S0167-2789(98)00266-8. http://linkinghub.elsevier.com/retrieve/pii/S0167278998002668

18. Toutant, A., Chandesris, M., Jamet, D., Lebaigue, O.: Jump conditions for filtered quantities at an under-resolved discontinuous interface. Part 1: theoretical development. Int. J. Multiphase Flow **35**(12), 1100–1118 (2009). http://www.sciencedirect.com/science/article/pii/S030193220900130X

19. Toutant, A., Chandesris, M., Jamet, D., Lebaigue, O.: Jump conditions for filtered quantities at an under-resolved discontinuous interface. Part 2: a priori tests. Int. J. Multiphase Flow **35**(12), 1119–1129 (2009). http://www.sciencedirect.com/science/article/pii/S0301932209001293

20. Toutant, A., Labourasse, E., Lebaigue, O., Simonin, O.: DNS of the interaction between a deformable buoyant bubble and a spatially decaying turbulence: a priori tests for LES two-phase flow modelling. Comput. Fluids **37**(7), 877–886 (2008). http://www.sciencedirect.com/science/article/pii/S004579300700165X

21. Vallet, A., Borghi, R.: An Eulerian model of atomization of a liquid jet. In: Proceedings of International Conference on Multiphase Flow, Lyon, France (1998)

22. Vallet, A., Burluka, A., Borghi, R.: Development of an eulerian model for the atomization of a liquid jet. Atom. Sprays **11**, 619–642 (2001)